The Journal of Experimental Biology 204, 2239–2250 (2001)
Printed in Great Britain © The Company of Biologists Limited 2001
JEB3466

SPATIAL VARIATION IN FAST MUSCLE FUNCTION OF THE RAINBOW TROUT *ONCORHYNCHUS MYKISS* DURING FAST-STARTS AND SPRINTING

D. J. ELLERBY* AND J. D. ALTRINGHAM

School of Biology, University of Leeds, Leeds LS2 9JT, UK

*Author for correspondence at present address: Department of Biology, 414 Mugar, Northeastern University, Boston, MA 02115, USA (e-mail: dellerby@lynx.neu.edu)

Accepted 17 April 2001

Summary

Fish fast-starts and sprints are rapid kinematic events powered by the lateral myotomal musculature. A distinction can be made between fast-starts and sprint-swimming activity. Fast-starts are kinematic events involving rapid, asymmetrical movements. Sprints involve a series of symmetrical, high-frequency tailbeats that are kinematically similar to lower-frequency, sustained swimming. The patterns of muscle recruitment and strain associated with these swimming behaviours were determined using electromyography and sonomicrometry. Axial patterns of fast muscle recruitment during sprints were similar to those in slow muscle in that the duration of electromyograhic (EMG) activity decreased in a rostro-caudal direction. There was also an axial shift in activity relative to the strain cycle so that activity occurred relatively earlier in the caudal region. This may result in caudal muscle performing a greater proportion of negative work and acting as a power transmitter as well as a power producer. The threshold tailbeat frequency for recruitment of fast muscle differed with location in the myotome. Superficial muscle fibres were recruited at lower tailbeat frequencies and shortening velocities than those deeper in the musculature. During sprints, fast muscle strain ranged from ±3.4 % l_0 (where l_0 is muscle resting length) at 0.35*FL* (where *FL* is fork length) to ±6.3 % l_0 at 0.65*FL*. Fast-starts involved a prestretch of up to 2.5 % l_0 followed by shortening of up to 11.3 % l_0. Stage 1 EMG activity began simultaneously, during muscle lengthening, at all axial locations. Stage 2 EMG activity associated with the major contralateral contraction also commenced during lengthening and proceeded along the body as a wave. Onset of muscle activity during lengthening may enhance muscle power output.

Key words: fast muscle, rainbow trout, *Oncorhynchus mykiss*, fast-start, electromyography, sonomicrometry, swimming, locomotion.

Introduction

Fish fast-starts and sprints are rapid kinematic events powered by the lateral myotomal musculature. The level of performance in this type of rapid manoeuvre is of direct survival value to the fish, both in terms of prey capture and in terms of predator avoidance. The majority of the lateral muscle is made up of fast anaerobic muscle fibres which power these rapid unsustained movements (e.g. Hudson, 1973; Bone, 1978; Jayne and Lauder, 1993). A distinction can be made between fast-starts and sprint swimming. Fast-starts are kinematic events involving rapid asymmetrical movements of the body. Kinematically, fast-starts are divided into two stages. Stage 1 represents the first muscular contraction when the body is typically thrown into a C or S curve. This stage ends when the contralateral contraction starts. Stage 2 is the return sweep of the tail blade. This produces rapid acceleration of the body (e.g. Webb, 1975; Webb, 1978; Harper and Blake, 1990). Sprints involve a short series of symmetrical, high-frequency tailbeats that are kinematically similar to lower-frequency sustained swimming. Fast-starts are associated with activity in the Mauthner neurones or M-cells, a pair of giant reticulospinal neurones. The axon of the M-cell decussates and synapses with motor neurones that innervate the lateral body musculature (Fetcho, 1991; Fetcho, 1992). M-cell activity can be initiated by auditory, visual or lateral-line stimuli (Canfield and Rose, 1993). Eaton et al. (Eaton et al., 1984) found that escape responses could also be initiated by non-Mauthner neuronal pathways.

The structure of the lateral musculature is complex. Axially, it is divided into a series of segmentally arranged myotomes. Each myotome is bounded by collagenous myosepta, which act as attachment points for the muscle fibres. The myotomes form a series of nested cones. Muscle fibre orientations in the superficial muscle lie approximately parallel with the body axis, although further from the body surface this is not the case. In most teleosts, the muscle fibres follow helical trajectories. Salmonids are an exception in that the trajectories are not helical but run from anterior to posterior cones of the myotomes, or from myotomal cones to the vertebral column (Alexander, 1969). Patterns of innervation are also complex. Hudson (Hudson, 1969) identified 12 motor units within a single myotome. In the majority of teleosts, fast muscle fibres

are multiply innervated, and each fibre has more than one motor end plate (Barets, 1961; Hudson, 1969), the number of which varies with position in the myotome (Altringham and Johnston, 1981). In addition, any given fibre may be innervated by axons from several adjacent spinal nerves (Hudson, 1969).

The fast myotomal muscle powers a diversity of swimming behaviours that encompass a wide range of swimming speeds and body kinematics. These require a range of strains and shortening velocities. The division between slow muscle activity at low speeds and fast muscle activity at higher speeds is well established (e.g. Rayner and Keenan, 1967; Bone, 1978; Rome et al., 1984; Jayne and Lauder, 1993). The underlying neuroanatomy may provide the scope for complex patterns of muscle activity within the fast muscle. There is little information on the muscle recruitment patterns within the complex three-dimensional architecture of the myotome. Jayne and Lauder (Jayne and Lauder, 1995) showed that, in largemouth bass (*Micropterus salmoides*) during burst-and-glide swimming, muscle activity in the extreme hypaxial and epaxial portions of the myotome could be decoupled from activity in the central portion. It seems likely that that there is variability in muscle recruitment within the myotome during different swimming behaviours. Electromyography was used to determine the patterns of muscle recruitment during fast-starts and sprint swimming in the rainbow trout *Oncorhynchus mykiss*. Recruitment patterns were determined both along the body axis and within a single myotome. The relationship between muscle activation and length is crucial in determining the patterns of power output. Simultaneous sonomicrometry was used to measure muscle length changes. This information is required if subsequent measurements of power output are to be made using the work loop technique (Josephson, 1985).

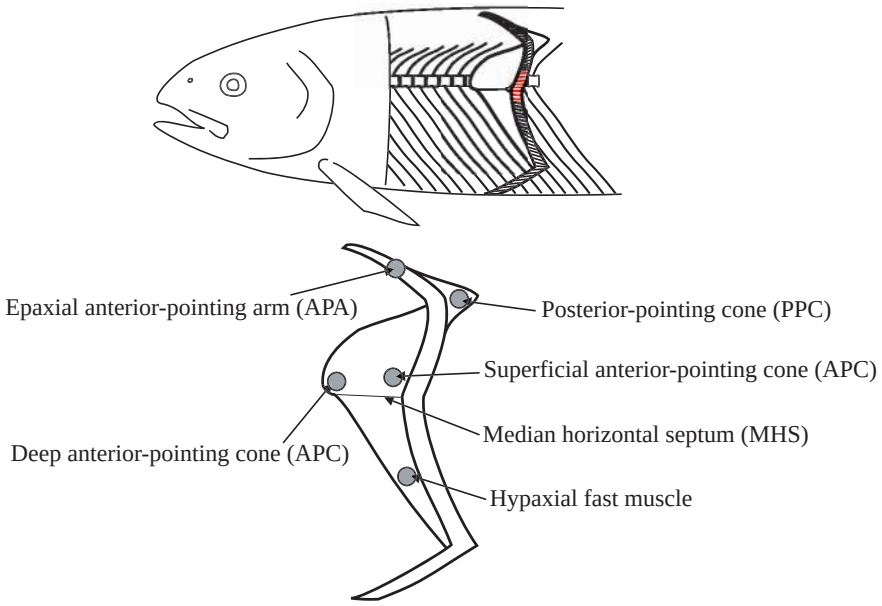

Fig. 1. Myotome 15 of the rainbow trout *Oncorhychus mykiss*. The surrounding myotomes have been removed to reveal its structure and relationship to the axial skeleton. Fibres tended to be oriented so that they were directed towards the apices of the anterior- and posterior-pointing cones. The circles indicate the locations of the measurement points.

Materials and methods

Rainbow trout, *Oncorhychus mykiss* (Walbaum), were purchased from Washburn Valley Trout Farm, North Yorkshire, UK. Fish were maintained at 14 °C in a circular tank 2 m in diameter and 1 m in depth. Water was aerated and recirculated through biological filters. Fish were exposed to a 16 h:8 h light:dark photoperiod and fed a diet of commercial trout pellets *ad libitum*. The mean fork length (*FL*) of the fish was 332±10 mm (range 295–354 cm, *N*=24). Mean mass was 342±11 g (range 290–392 g). All swimming experiments were conducted at 14 °C in a static tank 5.0 m long, 1.0 m wide and 1.0 m in depth.

Sonomicrometry and electromyography

The locations of measurement points are shown in Fig. 1. Table 1 details the muscle fibre orientations at these points. Four different approaches were used to gather muscle recruitment and strain data. In the first group of fish (*N*=6), electromyographic (EMG) and sonomicrometry recordings were made from three superficial points in the lateral fast muscle. These were at 0.35, 0.5 and 0.65*FL* (proportion of fork length from the snout). In a second group (*N*=6), EMG and sonomicrometry recordings were made from three sites in myotome 15. This was the fifteenth myotome posterior to the margin of the operculum. The first caudal vertebra was located at 0.59*FL* from the snout. This placed the measurement point at 0.65*FL* within the caudal region, whilst the remainder of the measurement points were in the trunk region. The superficial, lateral portion of myotome 15, where the median horizontal septum (MHS) meets the skin, was located at 0.35*FL*. The sites within the myotome were the posterior-pointing cones (PPCs), deep in the anterior-pointing cones (APCs) close to the vertebral column and the hypaxial muscle surrounding the body cavity. In two further groups (*N*=6 for each group), simultaneous recordings were obtained for a given site in myotome 15 on both sides of the fish and from a point in the slow muscle at 0.35*FL*. In one group, the fast muscle measurement site in myotome 15 was the superficial APC and in the second group it was the epaxial anterior-pointing arm (APA).

Sonomicrometry determines length changes from the transit time of an ultrasonic pulse between pairs of piezoelectric crystals. Measurements were made with a Triton Technologies

Table 1. *Fast muscle fibre orientation at the measurement points*

Position	Height of entry point relative to lateral line (mm)	Depth of anterior end of fibre (mm)	Fibre length (mm)	Angle relative to vertical septum (degrees)	Angle relative to MHS (degrees)
0.35*FL*, superficial anterior-pointing cone	6.0	7.0	5.4±0.1	11±0.5	18±0.8
0.50*FL*, superficial anterior-pointing cone	5.5	6.0	5.2±0.2	15±0.8	16±0.5
0.65*FL*, superficial anterior-pointing cone	5.0	4.3	4.8±0.1	19±0.7	15±0.5
Deep anterior-pointing cone	5.0	14.0	6.5±0.2	24±0.8	0±0.5
Posterior-pointing cone	17.0	8.0	4.8±0.1	−28±0.9	9±0.5
Epaxial anterior-pointing arm	24.0	4.0	3.6±0.1	10±0.6	0±0.5
Hypaxial fast muscle	−20	2.2	4.6±0.1	10±0.5	33±0.5

Positive angles relative to the vertical septum indicate that the fibres were angled outwards from the long axis posteriorly, negative angles indicate that the fibres were angled inwards posteriorly. Fibres at all location were either parallel to the median horizontal septum (MHS, Fig. 1) or angled away from it posteriorly.

Height of entry point refers to the entry point of the anterior needle for sonomicrometry crystal placement during surgery (positive measurements are above the lateral line). The anterior needle was set to the depth of the anterior end of the muscle fibre.

Values are means ± S.E.M. (N=6).

FL, fork length.

model 120-1000 sonomicrometer. The crystals were disc-shaped, with a diameter of 1.0 mm and a thickness of 0.3 mm (Triton Technologies type SL5-2). Crystals were implanted *via* 17 gauge hypodermic needles. Calibration of the crystals was carried out by direct measurement in fresh water. The transmission speed of ultrasound is slightly faster in muscle (1522–1572 m s^{-1}) than in water (1500 m s^{-1}), so a small correction had to be made (Goldman and Richards, 1954; Moi and Breddels, 1982). Changes in muscle density during contraction have little effect on the velocity of ultrasound (Griffiths, 1987; Hatta et al., 1988). The disc-shaped crystals are directionally sensitive. To ensure a clear signal, the flat faces of crystal pairs need to be facing each other. Pairs of needles were clamped together in the same plane and at the desired spacing to ensure correct alignment of the crystal pairs. The distance between the needles was equal to the mean fibre length at the sampling point (Table 1). All crystal leads and EMG electrodes were fitted with a 5 mm crossbar made from nylon monofilament fishing line. This was attached with epoxy resin. The crossbar was sutured to the skin to hold the wires in place and at the correct depth in the lateral muscle. The bar was arranged parallel to the face of the sonomicrometry crystal to indicate correct alignment.

An EMG electrode was implanted 3 mm dorsal to each pair of crystals. The bipolar electrodes were constructed from 0.125 mm diameter Teflon-coated silver wire (World Precision Instruments AGT 0510). The spacing of the recurved electrode tips was 1.0 mm, and the exposed portions of the tips were 1.5 mm in length. EMG signals were filtered and amplified using a CED 1902 signal conditioner. Amplifier gain was set at 1000 for each channel. A 50 Hz notch filter was applied to remove mains interference. EMG data were filtered digitally using Spike 2 software to apply a 100 Hz high-pass filter and a 1500 Hz low-pass filter. EMG electrodes and sonomicrometry crystals were linked to the preamplifiers by 5 m lengths of bathythermograph wire (Sippican Ocean Systems, Marion, MA, USA). All solder joints were cleaned with concentrated phosphoric acid prior to soldering. Phosphoric acid was also used as a flux in combination with a fluxless solder. All exposed solder joints were waterproofed using Dip-it Fantasy Film (Dip Film Products, UK).

Data channels were fed to a PC using a CED1401plus A/D converter and interface card. Data were recorded using Spike for Windows version 2.24.

Surgical procedures

Experimental animals were removed from the main holding tank using a net. A solution of MS 222 was used to anaesthetise the fish. Initial induction of anaesthesia was carried out by immersing the fish in a tank containing MS 222 at a concentration of 100 mg l^{-1}. Once the fish had clearly lost equilibrium (usually within 1 min), it was transferred to an operating table. This consisted of a length of polyvinylchloride guttering lined with wetted polyurethane foam. Anaesthesia was maintained with a less concentrated anaesthetic solution (MS 222, 37.5 mg l^{-1}), which was aerated and recirculated over the fish's gills using a submersible pump. The flow rate of the anaesthetic solution was 1.0 l min^{-1}. Surgical duration ranged from approximately 10 to 30 min. Minimising the time under anaesthesia reduced recovery times. In almost all cases, the fish recovered equilibrium within 2 min of being placed in the static tank. Restoration of the startle response took a further 5–10 min. Fish were left for a further 4 h to recover before data collection began.

Prior dissection had established the desired placements for the crystals and EMG electrodes in the myotomal muscle. The pectoral fin and lateral line were used as external markers to indicate correct placement during surgery. Fish were killed at the conclusion of each experiment by decapitation and pithing. Crystals and electrodes were dissected out to establish whether

they had been placed in the desired region of the myotome and were correctly aligned with the muscle fibres. Points where alignment of the sonomicrometry crystals was greater than 10° out from the fibre long axis, or where the crystals and electrodes were not placed in the desired portion of the myotome, were excluded from the analysis.

Video recording and kinematic analysis

Experiments were recorded using a NAC 400 high-speed video camera. This was mounted above the tank. At a frame rate of 200 frames s^{-1}, the field of view was approximately 2.0 m×1.4 m. The height of the field of view was halved at a frame rate of 400 frames s^{-1}. An ATI All-in Wonder Pro video card and software were used to grab video frames for kinematic analysis. Frames were grabbed at a resolution of 640 pixels×480 pixels. This meant that measurements could be made to an accuracy of approximately 3 mm. The frame rate of 400 Hz gave a time resolution of 0.0025 s. Measurements were made from still frames using Sigma Scan Pro image-analysis software.

During bursts of swimming, the stride length and tailbeat amplitude of the fish were measured. Stride length is the distance travelled by the fish during one complete tailbeat cycle. During fast-starts, the displacement of the centre of mass of the fish during kinematic stage 1 and stage 2 of the fast-start was measured. The centre of mass of a trout lies at 0.38*FL* (Webb, 1978). A marker was placed on the dorsal surface of the trout at this point. This consisted of a loop of suture thread marked with white paint. Displacement provides an accurate measure of performance compared with other parameters such as acceleration and velocity as it is least subject to computational error (Webb, 1978). The angle turned during the fast-start was also measured.

Statistical analyses

Sigma Stat (SPSS, Chicago, IL, USA) software was used for statistical analyses. Sprinting involved an initial acceleration phase. During sprints, analysis was restricted to the centre tailbeat of a sequence of five steady tailbeats. A sequence was considered steady if the tailbeat period and the swimming speed of the fish did not change by more than 10 % between the first and fifth tailbeat. Kinematic parameters of wired and unwired fish were compared using a Student's *t*-test. A Pearson product moment correlation was used to test for any relationships between muscle strain and activity and tailbeat frequency. A two-way analysis of variance (ANOVA) was used to test for significant differences in muscle strain and phase of activation between different locations in the musculature. The factors considered were either strain or activation, position within the musculature (either axial location or position within myotome 15) and individual. The position of the measurement site was considered to be a fixed factor, whilst all other factors were considered to be random. All results are expressed as means ± S.E.M., with the number of observations given in parentheses.

Results

Kinematic analysis

Sprint swimming

The presence of EMG electrodes and sonomicrometry crystals had no apparent effects on sprint swimming performance. There was no significant difference in stride length between wired and unwired fish during sprint swimming (P=0.58, Student's t-test). Mean stride length in wired fish was 0.67±0.02*FL* (N=20) compared with 0.68±0.02*FL* (N=20) in unwired fish. There was no significant relationship between stride length and tailbeat frequency (P=0.56, r=0.12, Pearson product moment correlation). During sprint swimming, the peak lateral deflection of the tail tip (D; proportion of *FL*) showed a significant positive correlation with tailbeat frequency (f) (P=0.0004, r=0.88, Pearson product moment correlation). The relationship can be described by the following linear equation: D=(0.062±0.03)+(0.0036±0.0004)f (Fig. 2). Fish outlines during a typical sprint are shown in Fig. 3A.

Fast-starts

The movement of a fish during a typical C-start is shown in Fig. 3B. The duration of kinematic stage 1, the formation of the C-curve, was 65.1±3.8 ms (N=20) in wired fish and 63.7±3.0 ms (N=20) in unwired fish. The mean displacement of the centre of mass during kinematic stage 1 was 5.2±0.4 cm (N=20) and 5.0±0.4 cm (N=20) in wired fish and unwired fish respectively. There was no significant difference in the fast-start performance of wired and unwired fish (Student's t-test, P=0.77 duration, P=0.63 displacement). A fast-start was typically preceded by a rapid straightening of the body or a

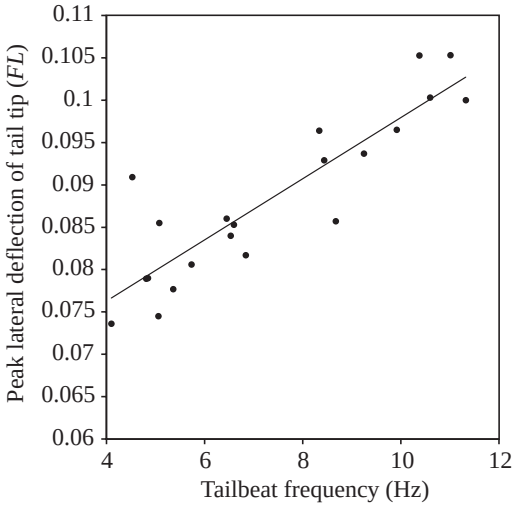

Fig. 2. The relationship between peak lateral deflection of the tail tip and tailbeat frequency. Peak deflection was measured as the perpendicular distance to the swimming track during straight-line swimming. Each data point represents a steady swimming sequence from a different unwired individual (N=20). *FL*, fork length. See text for further details.

slight curvature of the body to the side contralateral to the first major muscle contraction. All fast-starts were initiated with the body in a straight position. This can be seen in Fig. 3B, where the tail shows a small initial displacement in the direction opposite to the C-curve, highlighted in red. The change in direction of the fish during fast-starts was quantified. This was measured as the angle between a line from the tip of the fish's snout that bisected the head at rest and a similar line drawn at the completion of kinematic stage 1 and subsequently on completion of kinematic stage 2. Changes in direction during stage 1 ranged from 3 to 123°. There was a significant relationship between the angle of turn and the duration of kinematic stage 1 (Pearson product moment correlation, $P=4.9\times10^{-5}$, $r=0.78$). The mean change in direction during stage 2 was small compared with that during stage 1 (8.0±1.0°, $N=18$, compared with 58.0±9.0°, $N=18$).

Strain patterns

Sprint swimming

During sprint swimming, there was no significant relationship between superficial fast-muscle strain and tailbeat frequency (f) at 0.35*FL* ($P=0.75$, $r=-0.06$, Pearson product moment correlation) and 0.50*FL* ($P=0.82$, $r=-0.05$, Pearson product moment correlation). Overall, at 0.65*FL*, there was a significant relationship between muscle strain and tailbeat frequency, with strain showing a slight increase with increasing f ($P=0.03$, $r=0.52$, Pearson product moment correlation, Fig. 4). The relationship between muscle strain (s) and tailbeat frequency can be described by the following equation: $s=0.09f+5.62$. If the data for individual fish are considered separately, then only two of the six individuals showed a significant relationship between strain and tailbeat frequency. Representative recordings from a sequence of sprint swimming are shown in Fig. 5.

A two-way ANOVA was used to test for significant differences in muscle strain between different points in the fast muscle. There was no significant difference in the muscle strain between different fish at a given axial position (two-way ANOVA, $P=0.44$, $F=0.93$, d.f.=5). Muscle strain differed significantly with axial location (two-way ANOVA, $P<0.001$, $F=60.4$, d.f.=2). All pairwise comparisons were significantly different (Student–Newman–Keuls test, $P<0.05$). Strain increased along the body axis from anterior to posterior (Table 2). For strain measurements obtained from within the same myotome at 0.35*FL*, there was no significant difference in strain between fish for a given location (two-way ANOVA, $P=0.59$, $F=0.71$, d.f.=4). Strain did differ significantly with position within the myotome (two-way ANOVA, $P<0.001$, $F=148$, d.f.=2). All pairwise comparisons were significantly different (Student–Newman–Keuls test, $P<0.05$, Table 2). Strain was lower deeper in the myotome than in the more superficially placed measurement points.

Fast-starts

Muscle strains during fast-starts are shown in Table 3. The initial stages of the fast-start did not simply involve shortening associated with the formation of the C-curve. There was typically a small increase in muscle strain prior to the major muscle shortening. Because of the asymmetry of the strain cycle, the degree of lengthening and the degree of shortening are considered separately rather than the mean strain amplitude about l_0 (muscle resting length). There were significant differences in strain at different axial positions (two-way ANOVA, $P<0.001$, $F=46.8$, degree of lengthening; $P<0.001$, $F=39.9$, degree of shortening, d.f.=2), but not between fish for a given axial position (two-way ANOVA, $P=0.086$, $F=2.1$, degree of lengthening; $P=0.886$, $F=0.28$, degree of shortening, d.f.=4). Pairwise comparison between positions was made using the Student–Newman–Keuls method. The degree of fast muscle lengthening and shortening in the superficial APC at 0.65*FL* was significantly greater than at the other axial positions.

The timings of the starts of the strain cycles at 0.35, 0.50 and 0.65*FL* were measured relative to the first detectable movement of the tail tip. These times did not differ

Table 2. *Mean fast muscle strain during sprint swimming*

Position	% Strain ±l_0
0.35*FL*, superficial APC	3.4±0.07 (30)
0.50*FL*, superficial APC	4.1±0.08 (30)
0.65*FL*, superficial APC	6.3±0.08 (30)
Deep APC (myotome 15)	2.2±0.05 (25)
Posterior-pointing cone (myotome 15)	2.8±0.05 (25)
Hypaxial fast muscle (myotome 15)	3.3±0.06 (25)

Muscle strains are expressed as ± percentage of the muscle resting length l_0.

Means represent pooled data from more than one individual. Data were obtained from six fish in the superficial anterior-pointing cones (APCs) and from five fish at all other locations. Five measurements were taken from each individual. Values are means ± S.E.M. (*N*).

FL, fork length.

Table 3. *Mean fast muscle strain during stage 1 of fast-starts*

Position	% Lengthening	% Shortening
0.35*FL*, superficial APC	2.01±0.03 (25)[1]	9.23±0.25 (25)[2]
0.50*FL*, superficial APC	2.02±0.07 (25)[1]	9.51±0.19 (25)[2]
0.65*FL*, superficial APC	2.54±0.04 (25)	11.26±0.28 (25)
Deep APC (myotome 15)	1.26±0.06 (25)	6.91±0.33 (25)
Posterior-pointing cone (myotome 15)	1.86±0.08 (25)[1]	8.76±0.38 (25)[2]
Hypaxial fast muscle (myotome 15)	1.78±0.15 (25)[1]	8.82±0.45 (25)[2]

Strains are expressed as ± percentage of the muscle resting length l_0.

Muscle strains marked with the same superscripted number are not significantly different (two-way ANOVA, $P>0.05$).

Data are from five fish, five measurements were taken from each individual. Values are means ± S.E.M. (*N*).

APC, anterior-pointing cone.

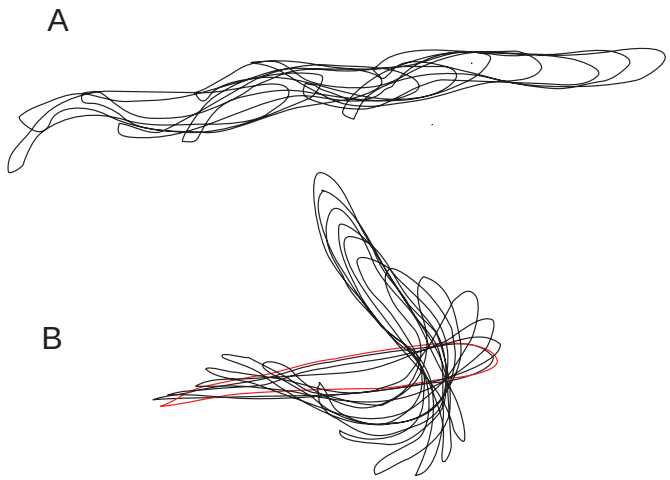

Fig. 3. Fish outlines during sprinting (A) and a C-start (B). Outlines were traced at 20 ms intervals during sprinting and at 10 ms intervals during the C-start. The outline highlighted in red shows the small initial movement contralateral to the C-curve.

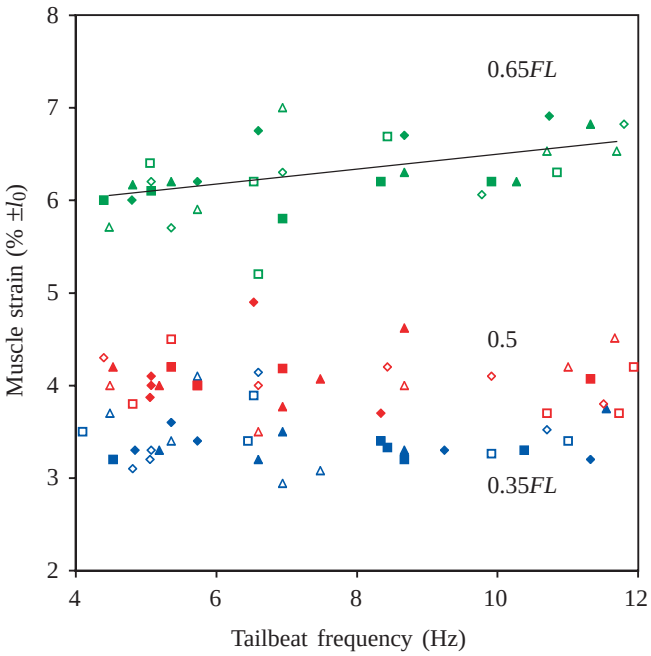

Fig. 4. Muscle strain in the superficial anterior-pointing cones at three points along the body during sprint swimming. Strain is expressed as the percentage length change $\pm l_0$, where l_0 is muscle resting length. Blue, red and green points represent data from 0.35, 0.5 and 0.65*FL* respectively, where *FL* is fork length. Values from different fish are shown with different symbols. Data are from six fish, with five measurements from each individual. The solid line is the significant relationship for 0.65*FL* (see text for further details).

significantly with body position (two-way ANOVA, P=0.315, F=0.17, d.f.=2). On this basis, onset of the strain cycle was considered to be synchronous at all points along the body. Despite this, there was a clear time lag in the attainment of minimum muscle length along the length of the body axis, and

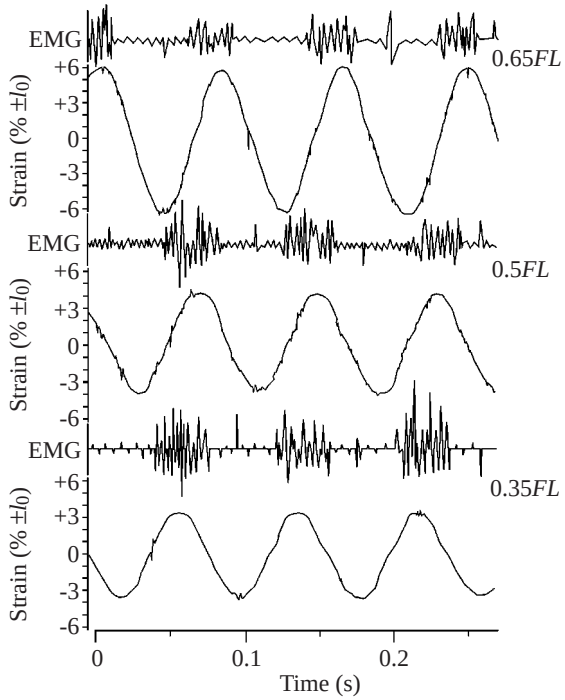

Fig. 5. Representative fast muscle strain and EMG traces from three points along the body axis during sprinting at approximately 12 Hz. Measurements were taken at 0.35, 0.5 and 0.65*FL*, where *FL* is fork length, from the snout in the superficial anterior-pointing cones of the myotome. Strain is expressed as the percentage length change $\pm l_0$, where l_0 is muscle resting length.

the speed of the wave of muscle shortening was calculated from this time lag. The mean velocity of the strain wave measured from the points of minimum muscle fibre length along the body was 17.9±0.6*FL* s^{-1} (N=6).

Within myotome 15 at 0.35*FL*, for a given position, there was no significant difference in strain in different fish during muscle lengthening (two-way ANOVA, P=0.652, F=0.62, d.f.=4). However, one individual did show significantly lower strains during muscle shortening (two-way ANOVA, P=0.011, F=3.6, d.f.=4). There were significant differences in strain between different locations within the myotome (two-way ANOVA, P<0.001, F=52.6, degree of lengthening; P<0.001, F=102, degree of shortening, d.f.=2). The degree of fast muscle lengthening and shortening was significantly lower in the deep APC than in the other more superficial positions in myotome 15 (Table 3).

Activation patterns

Slow muscle activity

EMG activity was detected from slow muscle during sprint swimming at all tailbeat frequencies and during fast-starts.

Sprint swimming

Strain patterns in sprint swimming were approximately sinusoidal and can be described using a 360° cycle. The relationships between phase of EMG activity and the muscle

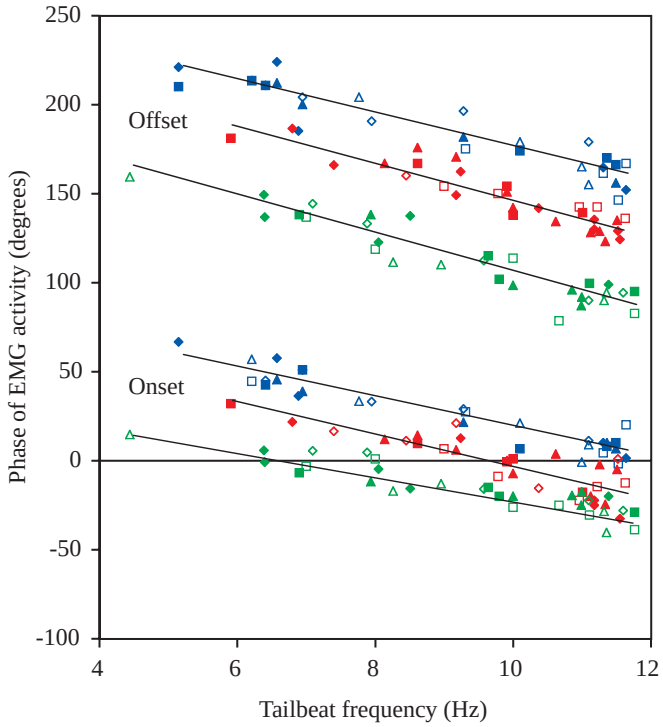

Fig. 6. The relationship between phase of EMG activity and tailbeat frequency during sprinting. Onset and offset times of EMG activity are relative to the sinusoidal, 360 °, strain cycle. Muscle is at resting length l_0 at 0 ° and maximum length at 90 °. Blue, red and green points represent data from 0.35, 0.5 and 0.65*FL*, respectively, where *FL* is fork length. Values from different fish are shown with different symbols. Data are from six fish, with five measurements from each individual. Equations for the lines are presented in Table 4.

strain pattern at three points along the body are shown in Fig. 6. The only portions of the myotome consistently active during sprint swimming were the superficial APCs and the hypaxial fast muscle. The onset of EMG activity relative to the strain cycle occurred progressively earlier moving in a rostro-caudal direction. There was a significant difference in EMG duration relative to the strain cycle with axial position during sprint swimming (two-way ANOVA, $P<0.001$, $F=72.9$, d.f.=2). EMG duration became significantly shorter moving in a caudal direction. Mean EMG duration (pooled data for six fish) was 159±1.4 ° ($N=30$) at 0.35*FL*, 150±1.9 ° ($N=30$) at 0.5*FL* and 128±2.4 ° ($N=30$) at 0.65*FL*. The EMG duration relative to the strain cycle did not change significantly with tailbeat frequency (Table 4). The mean tailbeat frequency at which fast muscle EMG activity was first detected in fast muscle, at a range of locations, is shown in Table 5. There were significant differences in the tailbeat frequency at which fast muscle was initially recruited during sprint swimming at different locations within the myotome (two-way ANOVA, $P<0.001$, $F=82.2$, d.f.=3). The APAs remained inactive during sprint swimming. The superficial APCs and the hypaxial fast muscle were recruited at lower tailbeat frequencies than the PPCs (Fig. 7).

Table 4. *Relationships between EMG activity patterns and tailbeat frequency during sprint swimming*

Variable	Linear equation	Correlation coefficient, *r*
EMG onset 0.35*FL*	=(99.9±4.7) – (8.2±0.5)*f*	–0.95*
EMG onset 0.50*FL*	=(88.0±10.5) – (9.1±1.0)*f*	–0.85*
EMG onset 0.65*FL*	=(42.8±5.1) – (6.2±0.5)*f*	–0.91*
EMG offset 0.35*FL*	=(277.0±6.4) – (10.3±0.1)*f*	–0.94*
EMG offset 0.50*FL*	=(253.4±8.5) – (10.7±0.8)*f*	–0.92*
EMG offset 0.65*FL*	=(210.5±7.0) – (10.5±0.7)*f*	–0.94*
EMG duration 0.35*FL*	=(168.1±5.4) – (1.0±0.6)*f*	–0.32
EMG duration 0.50*FL*	=(165.4±12.9) – (1.5±1.3)*f*	–0.22
EMG duration 0.65*FL*	=(167.8±8.9) – (4.3±0.9)*f*	–0.35

Correlation coefficients marked with an asterisk denote a statistically significant relationship between the variables ($P<0.05$, Pearson product moment correlation).

f, tailbeat frequency; *FL*, fork length.

Table 5. *Mean tailbeat frequency during sprint swimming at which EMG activity was detected in the fast muscle of myotome*

Position	Threshold tailbeat frequency during sprints (Hz)
Superficial APC	4.8±0.1[1]
Deep APC	9.1±0.8
PPC	8.3±0.2
APA	Inactive
Hypaxial fast muscle	5.0±0.3[1]

Frequencies that are not significantly different are marked by the same number ($N=6$).

Values are means ± S.E.M.

APC, anterior-pointing cone; PPC, posterior-pointing cone; APA, anterior-pointing area.

Fast-starts

Because of the asymmetrical movements involved in fast-starts, it is not appropriate to describe them using a 360 ° strain cycle. The EMG activity associated with the first major muscular contraction is referred to as the stage 1 EMG burst, and EMG activity associated with the successive contralateral contraction is referred to as the stage 2 EMG burst. The stage 1 EMG burst was preceded by a preliminary EMG burst (Fig. 8).

There was a significant linear relationship between the change in direction during stage 1 of a fast-start and the duration of the stage 1 EMG (Pearson product moment correlation, $P=4.4\times10^{-5}$, $r=0.78$). There was also a significant linear relationship between the duration of stage 1 and the duration of the stage 1 EMG (Pearson product moment correlation, $r=0.67$, $P<0.05$). The proportion of stage 1 taken up by EMG activity remained relatively constant regardless of turning angle or stage 1 duration and had no significant correlation with change in direction (Pearson product moment

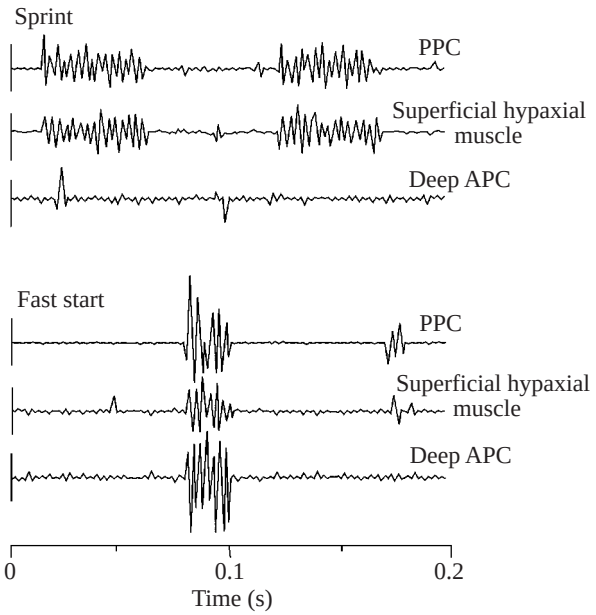

Fig. 7. Fast muscle EMG activity in the posterior-pointing cones (PPCs), the hypaxial muscle and the deep anterior-pointing cones (APCs) of myotome 15. Traces show sprinting at 10 Hz and the stage 1 EMG of a fast-start, both in the same fish.

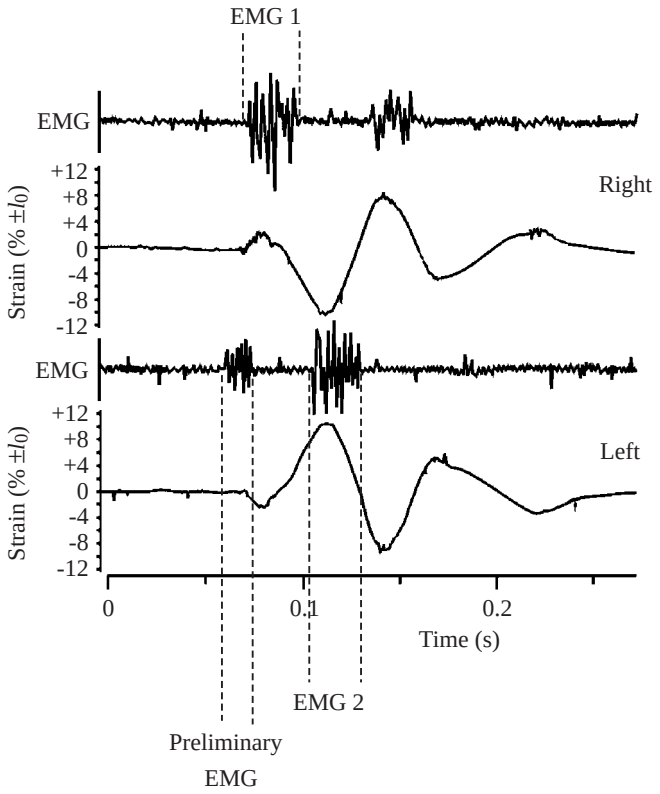

Fig. 8. Simultaneous strain and EMG recordings from the superficial anterior-pointing cones of myotome 15 on both sides of a trout during a fast-start. Strain is expressed as the percentage length change ±l_0, where l_0 is muscle resting length.

correlation, P=0.08, r=0.11) or with stage 1 duration (Pearson product moment correlation, P=0.54, r=–0.15).

To determine whether there was a wave of EMG progression during stage 1 of the fast-start, the time of maximum muscle length at 0.35*FL* during the first contraction of the fast-start was taken as a reference point. The timing of EMG activity along the body relative to this point was measured. During stage 1, the time differences between EMG onsets along the body and the reference point were not significantly different (two-way ANOVA, P=0.40, F=0.94, d.f.=2). EMG 1 duration did not differ significantly with axial location (two-way ANOVA, P=0.81, F=0.22, d.f.=2).

To determine whether there was a wave of EMG activity during stage 2, the time of maximum muscle length at 0.35*FL* was again taken as a reference point. There was a significant difference in the time lags between this reference point and the EMG onsets along the body (two-way ANOVA, P<0.001, F=74.3, d.f.=2). EMG onset occurred significantly later at 0.65*FL* than at 0.35*FL* (Student–Newman–Keuls, q=7.48, P<0.05) or 0.5*FL* (Student–Newman–Keuls, q=5.20, P<0.05). This suggests that there was a wave of muscle activity during stage 2 of the fast-start (Fig. 9).

There was a significant change in stage 2 EMG duration with axial location (two-way ANOVA, P<0.001, F=18.5, d.f.=2). There was no significant difference in EMG 2 duration between different fish for a given position (two-way ANOVA, P=0.999, F=0.02, d.f.=4). EMG 2 duration was significantly shorter at 0.65 than at 0.35*FL* (Student–Newman–Keuls, P<0.05, q=8.17) and 0.5*FL* (Student–Newman–Keuls, P<0.05, q=6.42). There was no significant difference in EMG 2 duration between 0.35 and 0.5*FL* (Student–Newman–Keuls, P>0.05, q=1.75). Pooled mean EMG 2 durations were 36.4±1.2, 34.7±0.9 and 28.4±0.8 ms (N=25) at 0.35, 0.5 and 0.65*FL* respectively.

At all positions, EMG 2 onset occurred before maximum muscle length. There was a shift in the onset of EMG 2 relative to the point of maximum muscle length with axial location (two-way ANOVA, P<0.001, F=64.7, d.f.=2). All pairwise comparisons were significantly different (Student–Newman–Keuls, P<0.05). EMG 2 onset occurred progressively earlier relative to the strain cycle moving along the body axis from anterior to posterior. There was no significant difference in EMG onset between different fish (two-way ANOVA, P=0.626, F=0.65, d.f.=4). EMG 2 onset occurred at 16.8±0.6 ms (N=25), 21.6±0.8 ms (N=25) and 27.9±0.6 ms (N=25) before maximum muscle length at 0.35, 0.5 and 0.65*FL* respectively (pooled mean data).

Discussion

Kinematics

A variety of manoeuvres involving very different degrees of body curvature can be powered by the fast muscle (Fig. 3). The speed of kinematic events also spans a wide range, from C-curves executed in 65 ms to tailbeats with a period of 250 ms. Fast-starts showed kinematic variation, especially during stage

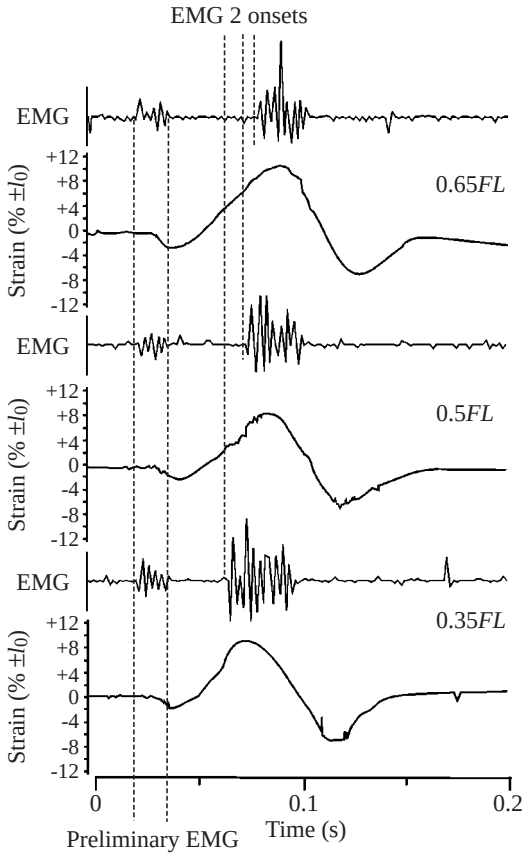

Fig. 9. The relationship between the strain cycle and EMG activity at three points along the body of a trout during stage 2 of a fast-start. Data were obtained from the superficial anterior-pointing cone of the myotome at 0.35, 0.5 and 0.65*FL*, where *FL* is fork length. Strain is expressed as the percentage length change ±l_0, where l_0 is resting muscle length.

1, in which the degree of turning was highly variable. Stage 2 was more stereotyped and appeared mainly to involve thrust generation. The straightening of the body prior to the C-curve coincided with an increase in muscle strain. In some respects, sprint swimming was similar to the swimming style adopted at low speeds and powered by slow muscle. Stride length (0.68*FL*) was similar to that previously measured in steadily swimming trout at lower velocities (Webb et al., 1984, 0.65*FL*; Hammond et al., 1998, 0.63*FL*). Tailbeat amplitudes fell within the range measured previously (Webb et al., 1984). Stride length did not change significantly with tailbeat frequency. This was also the case in saithe (*Pollachius virens*) and mackerel (*Scomber scombrus*) (Videler and Hess, 1984) and bluefin tuna (*Thunnus thynnus*; Wardle et al., 1989), in which stride length varied little over a wide range of swimming speeds. This contrasts with the results of many other studies, which show an increase in stride length with increasing swimming speed (e.g. Bainbridge, 1958; Hunter and Zweifel, 1971; Webb et al., 1984; Dewar and Graham, 1994). The major difference between the two groups of studies is that those showing little change in stride length were conducted in static tanks and those showing a marked change were conducted in flow tanks. It is possible that the flow conditions within flow tanks lead to changes in stride length as the imposed flow velocity increases.

Strain and shortening velocity

The speed of the strain wave along the body relative to the tailbeat cycle (1.2 $FL\,T^{-1}$) was similar to that measured in trout slow muscle by Hammond et al. (1998; 1.0 $FL\,T^{-1}$). Mean superficial fast muscle strains (increasing from ±3.4 % at 0.35*FL* to ±6.3 % at 0.65*FL*) were similar to those previously measured in the superficial slow muscle (increasing from ±3.0 % at 0.35*FL* to ±6.0 % at 0.65*FL*) during low-tailbeat-frequency swimming (Hammond et al., 1998). The increase in caudal muscle strain with increasing tailbeat frequency (Fig. 4) may be linked to a progressive change in swimming kinematics as tailbeat frequency increased. This was detected as an increase in the lateral deflection of the tail blade (Fig. 2). Within certain limits, increased muscle strain can result in increased power production (e.g. Ellerby et al., 2001) and may in part help to meet the greater power requirements of high-velocity swimming. Increased muscle strain has also been recorded in milkfish (*Chanos chanos*) (Katz et al., 1999) at high swimming velocities.

The measurements made within the same myotome were not precisely within the same transverse plane; however, the distance between the sampling points along the long axis of the fish was small (approximately 0.05*FL*), and the strain measurements gave an approximation of those within the same cross section (Fig. 1). Muscle strain was significantly lower in the deepest portion of the APC than in more superficial regions of the myotome during both sprints and fast-starts. There was no uniformity of strain across different depths of a given muscle cross section as predicted by Alexander (Alexander, 1969) on the basis of muscle fibre geometry. Although strain at different myotomal locations was not uniform, it did not change with chordwise distance as much as would be expected for longitudinally arranged fibres. In longitudinally arranged fibres in the same transverse plane, strain would be proportional to the chordwise distance of the fibre from the spine. If this were the case, then strain in the superficial APC would be approximately four times that in the deep APC, whilst the measured values were only 1.5 times greater.

Many important muscle properties (e.g. power output, efficiency) are dependent on the ratio V/V_{max}, where V is the shortening velocity of the muscle fibres and V_{max} is their maximal shortening velocity. Maximum superficial muscle shortening velocities have previously been measured in carp (*Cyprinus carpio*; Rome et al., 1990) and scup (*Stenotomus chrysops*; Rome et al., 1992). In the present study, the overall shortening velocity taken from peak to minimum length was calculated. As this includes periods of acceleration and deceleration, it will clearly be lower than the maximum velocity. As the strain waveform approximated a sine wave, the difference between maximum and overall shortening velocities can be calculated. The differential of a sine wave is

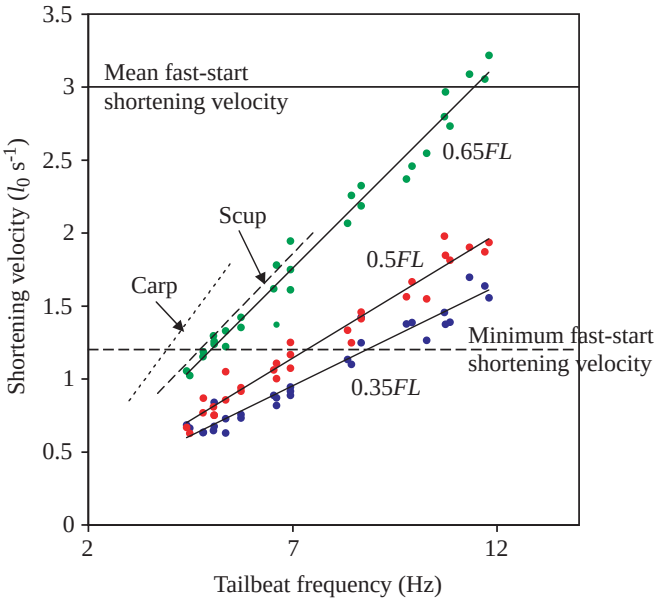

Fig. 10. Fast muscle shortening velocity at three points along the body axis during sprinting. Blue, red and green points represent data from 0.35, 0.5 and 0.65*FL*, respectively, where *FL* is fork length. Data for carp and scup were derived from Rome et al. (Rome et al., 1992). The solid horizontal line represents the mean fast-start muscle shortening velocity. The dashed horizontal line represents the minimum fast-start muscle shortening velocity. l_0 is the resting muscle length. r=0.99, 0.98 and 0.97 for linear regression lines at 0.35, 0.5 and 0.65*FL*, respectively. For all lines P<0.05 (Pearson product moment correlation).

a cosine. This means that, if the maximum shortening velocity is 1, then the overall shortening velocity will be $2/\pi$ or approximately 64 % of the maximum shortening velocity. A comparison can therefore be made between maximum and overall shortening velocities.

During sprinting, the shortening velocity increased with tailbeat frequency (Fig. 10). In carp, maximum muscle velocities ranged from 0.6 to 2.0 $l_0\,s^{-1}$ (where l_0 is the resting muscle length) over a tailbeat frequency range of 2.5–5.5 Hz (Rome et al., 1990). Scup maximum muscle velocities ranged from 0.8 to 1.8 $l_0\,s^{-1}$ over a tailbeat frequency range of 3.5 to 6.5 Hz (Rome et al., 1992). At 5.5 Hz, in trout, overall shortening velocities range from 0.7 to 1.3 $l_0\,s^{-1}$ (Fig. 10). This corresponds to an approximate maximum velocity range of 1.1–2.0 $l_0\,s^{-1}$. At an equivalent tailbeat frequency, superficial muscle shortening velocities were similar in carp, scup and trout.

Mean shortening velocities during stage 1 of fast-starts were generally higher than during sprints. Mean overall shortening velocities were 2.9±0.2, 3.0±0.1 and 3.0±0.2 $l_0\,s^{-1}$ (N=30) at 0.35, 0.5 and 0.65*FL*, respectively. However, shortening velocities measured during fast-starts ranged from 1.2 to 4.9 $l_0\,s^{-1}$. In terms of shortening velocity, there was considerable overlap in fast muscle function between the two types of swimming behaviour, although many fast-starts involved greater shortening velocities than those involved in sprinting.

At all points in the fast muscle that were examined, there was a small extension (1.3–2.5 % l_0) in muscle length prior to the major muscular contraction associated with the C-curve. This also appears to occur during fast-starts in other species. A similar, although smaller (1 % l_0), prestretch was detected by Franklin and Johnston (Franklin and Johnston, 1997) during fast-starts in the Antarctic rock cod (*Notothenia coriiceps*). A small prestretch is also discernible in some of the strain traces obtained during carp (*Cyprinus carpio*) fast-starts by Wakeling and Johnston (Wakeling and Johnston, 1999). Covell et al. (Covell et al., 1991) did not identify any prestretch in the trout prior to the main stage 1 muscle contraction. However, length was determined at a sampling rate of 200 Hz. This may have obscured the brief prestretch which, in the present study, was approximately 10 ms in duration from resting length to peak length (Fig. 8, Fig. 9). Franklin and Johnston (Franklin and Johnston, 1997) identified shortening of more anterior muscles as the source of the prestretch. If the onset of activity and shortening are synchronous, as in the trout, then this seems unlikely.

The degree of overall shortening (6.9–11.3 %) was similar to that found in trout by Covell et al. (Covell et al., 1991) (9.4 % shortening at 0.45*FL*, range 4.5–15.4 %). The onset of the strain cycle was simultaneous along the length of the body, but there was a delay in reaching minimum muscle length moving from anterior to posterior. The strain wave speed (17.9 $FL\,s^{-1}$) calculated from this progression was towards the upper end of the range of fast-start body curvature speeds measured by Wakeling and Johnston (Wakeling and Johnston, 1998; 4.17 $FL\,s^{-1}$ in *Notothenia coriiceps* to 24.45 $FL\,s^{-1}$ in *Serrana cabrilla*). This contrasts with the results of Covell et al. (Covell et al., 1991), who found that in trout the muscle reached minimum length approximately synchronously at anterior (0.45*FL*) and posterior (0.64*FL*) recording sites. The time lag is rather small (approximately 17 ms) even between 0.35 and 0.65*FL*. The closer placement of their sample points may have obscured the difference. The delay in reaching minimum length may be due to the change in muscle properties along the length of the fish; alternatively, or additionally, the resistance of the water may delay the movement of the caudal region of the body.

Activation patterns

Progressing caudally along the fish there was a clear negative shift in the onset of EMG activity relative to the strain cycle in the fast muscle (Fig. 5, Fig. 6). This was qualitatively similar to the pattern observed in the slow muscle of several species (for a review, see Altringham and Ellerby, 1999). This suggests a change in fast muscle function along the length of the body. A negative phase shift results in a greater proportion of negative work performed by the muscle (Altringham et al., 1993; van Leeuwen et al., 1990). This stiffens the muscle and may act to transmit power from more anterior muscle as well as producing power. This may be of particular importance in fast muscle, in which the bulk of the muscle is placed anteriorly, well away from the tail blade. Measurements of

axial fast muscle power outputs *in vitro* are required to establish whether this occurs in the trout.

The absolute duration of muscle activity decreased with increasing tailbeat frequency, but the duration of activity relative to the strain cycle remained approximately constant (Table 4). This was also the case in the sculpin (Johnston et al., 1993), in which duty cycle remained at around 110 °, and also in mackerel and saithe (Wardle and Videler, 1993). *In vitro*, the optimum duty cycle decreases as cycle frequency increases (Altringham and Johnston, 1990; Johnston et al., 1993; Hammond et al., 1998; Ellerby et al., 2001). As tailbeat frequency increases, the fast muscle fibres may be operating under increasingly sub-optimal stimulus conditions. Long duty cycles at high cycle frequencies prevent the the fibre from relaxing fully before the subsequent stimulus (Altringham and Johnston, 1990; Johnston et al., 1993). This results in a greater negative work component during the strain cycle and reduced overall power output.

The preliminary EMG burst may be the source of the prestretch in the lateral muscle prior to the muscle contraction associated with the C-curve. EMG activity contralateral to the C-curve and coincident with a small prestretch is apparent in the carp (see fig. 1 in Wakeling and Johnston, 1999), although it appears to be coincident with the stage 1 EMG rather than prior to it as in the present study. During the stage 1 contraction, muscle activity started during muscle lengthening (Fig. 8). Onset of muscle activity during this prestretch should enhance muscle force and power production during the subsequent shortening phase (Altringham and Johnston, 1990; Franklin and Johnston, 1997). Increased power production would be advantageous in increasing fast-start performance. Onset of stage 1 activity appeared to be simultaneous at all points along the body. This was also the case in the carp *Cyprinus carpio* (Wakeling and Johnston, 1999).

Kinematic stage 1 was a preparatory phase mainly dominated by turning. The turning angle was proportional to the length of the initial EMG burst. The duration of the stage 1 EMG may dictate the turning angle. Stage 1 EMG duration remained constant along the body. Stage 2 activity also started during muscle lengthening, although the overall pattern of stage 2 muscle activity was very different; a wave of activation passed along the body and EMG duration decreased posteriorly (Fig. 9). There was also shift in activity relative to the strain cycle so that more time was spent active during lengthening in the caudal than in the anterior muscle. In these respects, stage 2 exhibited similar activity patterns to those seen in sprint swimming and appeared to involve mainly thrust generation rather than turning. A direct comparison between the activation patterns during stage 2 and sprinting is difficult because of the asymmetry of the fast-start strain cycle. However, the range of mean EMG 2 durations (36 ms at 0.35*FL*, 28 ms at 0.65*FL*) was similar to that during a 12 Hz tailbeat frequency sprint (37 ms at 0.35*FL*, 30 ms at 0.65*FL*). The magnitude of the phase shift relative to peak muscle length was also similar. On average, onset of muscle activity occurred 17 ms before maximum length at 0.35*FL* and 28 ms before maximum length at 0.65*FL*. This compares with values of 16 and 28 ms at 0.35 and 0.65*FL*, respectively, during sprinting at 12 Hz.

Slow muscle activity was detected at all tailbeat frequencies during sprinting and also during fast-starts. Jayne and Lauder (Jayne and Lauder, 1993) also found that during fast-starts in bluegill sunfish (*Lepomis gibbosus*) both slow and fast muscle at a given longitudinal location were activated simultaneously. This is despite the fact that the *in vitro* performance of trout slow muscle suggests that it could not produce net positive power at tailbeat frequencies above 5 Hz (Hammond et al., 1998). It is possible that slow muscle EMG electrodes were detecting activity from the adjacent fast muscle fibres.

Recruitment of fast fibres was not an all-or-nothing event. During sprinting, there was evidence for increasing recruitment of fast muscle fibres as tailbeat frequency increased (Table 5; Fig. 7). Initial recruitment of fast muscle fibres occurred in the superficial anterior-pointing cones of the myotome and the superficial hypaxial muscle. As tailbeat frequency increased, additional fibres in the posterior-pointing cones and deeper in the anterior-pointing cones were recruited. Fibres in the anterior-pointing arms of the myotomes were only recruited during fast-starts. The power requirements of swimming scale to approximately the third power of swimming speed (Webb et al., 1984). The number of motor units recruited could apparently be increased to meet increasing power requirements. The underlying neuroanatomy may support this mechanism. In the zebrafish *Danio rerio*, separate motor neurones innervate different regions of the myotome (Westerfield et al., 1986), and Hudson (Hudson, 1969) showed that there were 12 motor units within each abdominal myotome of the short-horned sculpin. Altringham and Johnston (Altringham and Johnston, 1981) showed that deeper fast fibres in the cod (*Gadus morhua*) had fewer motor end plates than superficial fast fibres. They suggested that, for a given level of stimulation, this could lead to a lower level of activity in deep compared with superficial fibres. Innervation patterns in the trout have not been studied in detail, but a similar innervation pattern could provide a possible mechanism to allow differential fibre recruitment with depth.

The recruitment of deeper portions of the myotome at higher tailbeat frequencies and during fast-starts may not just be related to the increased power requirements of higher swimming speeds. The wide range of shortening velocities experienced by fast fibres could also be a factor. It is possible that the contractile properties of the deeper portions of the myotome are better suited to higher shortening velocities. There is evidence that myotomal slow muscle twitch times decrease with depth (Altringham and Block, 1997). It is not known whether fast muscle properties also change with depth. If the twitch kinetics of the fibres were faster at greater depth, they would be better suited to powering higher tailbeat frequencies. *In vitro* investigation of the intrinsic properties and power outputs of fast fibres at different myotomal locations is required to determine whether this is the case.

D.J.E. was supported by a BBSRC special studentship. The high-speed video camera was loaned by the EPSRC engineering instrument pool. We are grateful to two anonymous referees for their constructive criticism.

References

Alexander, R. McN. (1969). The orientation of muscle fibres in the myomeres of fish. *J. Mar. Biol. Ass. U.K.* **49**, 263–290.

Altringham, J. D. and Block, B. A. (1997). Why do tuna maintain elevated slow muscle temperatures: power output of muscle isolated from endothermic and ectothermic fish. *J. Exp. Biol.* **200**, 2617–2627.

Altringham, J. D. and Ellerby, D. J. (1999). Fish swimming: patterns in muscle function. *J. Exp. Biol.* **202**, 3397–3403.

Altringham, J. D. and Johnston, I. A. (1981). Quantitative histochemical studies of the peripheral innervation of cod (*Gadus morhua*) fast myotomal muscle fibres. *J. Comp. Physiol.* **143**, 123–127.

Altringham, J. D. and Johnston, I. A. (1990). Modelling muscle power output in a swimming fish. *J. Exp. Biol.* **148**, 395–402.

Altringham, J. D., Wardle, C. S. and Smith, C. S. (1993). Myotomal muscle function at different locations in the body of a swimming fish. *J. Exp. Biol.* **182**, 191–206.

Bainbridge, R. (1958). The speed of swimming as related to size and to the frequency and amplitude of tail beat. *J. Exp. Biol.* **40**, 23–56.

Barets, A. (1961). Contribution a l'étude des systèmes moteurs lent et rapide du muscle latéral des téléostéens. *Arch. d'Anat. Microsc. Morph. Exp.* **50**, 91–187.

Bone, Q. (1978). On the role of different fibre types in fish myotomes at intermediate swimming speeds. *Fish. Bull.* **76**, 691–699.

Canfield, J. G. and Rose, G. J. (1993). Activation of Mauthner neurons during prey capture. *J. Comp. Physiol. A* **172**, 611–618.

Covell, J. W., Smith, M., Harper, D. G. and Blake, R. W. (1991). Skeletal muscle deformation in the lateral muscle of the intact rainbow trout during fast-start manoeuvers. *J. Exp. Biol.* **156**, 453–466.

Dewar, H. D. and Graham, J. B. (1994). Studies of tropical tuna swimming performance in a large water tunnel. III. Kinematics. *J. Exp. Biol.* **192**, 45–59.

Eaton, R. C., Nissanov, J. and Wieland, C. M. (1984). Differential activation of Mauthner and non-Mauthner startle circuits in the zebrafish: Implications for functional substitution. *J. Comp. Physiol. A* **155**, 813–820.

Ellerby, D. J., Spierts, I. L. Y. and Altringham, J. D. (2001). Slow muscle power output of yellow- and silver-phase European eels (*Anguilla anguilla*, L.): changes in muscle performance prior to migration. *J. Exp. Biol.* **204**, 1369–1379.

Fetcho, J. R. (1991). Spinal network of the Mauthner cell. *Brain Behav. Evol.* **37**, 298–316.

Fetcho, J. R. (1992). Excitation of motoneurons by the Mauthner axon in goldfish: complexities in a simple reticulospinal pathway. *J. Neurophysiol.* **67**, 1574–1586.

Franklin, C. E. and Johnston, I. A. (1997). Muscle power output during escape responses in an Antarctic fish. *J. Exp. Biol.* **200**, 703–712.

Goldman, D. E. and Richards, J. R. (1954). Measurement of high frequency sound velocity in mammalian soft tissues. *J. Acoust. Soc. Am.* **26**, 981–983.

Griffiths, R. I. (1987). Ultrasound transit time gives direct measurment of muscle fibre length *in vivo*. *J. Neurosci. Meth.* **21**, 159–165.

Hammond, L., Altringham, J. D. and Wardle, C. S. (1998). Myotomal slow muscle function of rainbow trout *Oncorhynchus mykiss* during steady swimming. *J. Exp. Biol.* **201**, 1659–1671.

Harper, D. G. and Blake, R. W. (1990). Fast-start performance of rainbow trout *Salmo gairdneri* and Northern pike *Esox lucius*. *J. Exp. Biol.* **150**, 321–342.

Hatta, I., Sugi, H. and Tamura, Y. (1988). Stiffness changes in frog skeletal muscle during contraction recorded using ultrasonic waves. *J. Physiol., Lond.* **403**, 193–209.

Hudson, R. C. L. (1969). Polyneuronal innervation of the fast muscles of the marine teleost *Cottus scorpius* L. *J. Exp. Biol.* **50**, 47–67.

Hudson, R. C. L. (1973). On the function of white muscles in teleosts at intermediate swimming speeds. *J. Exp. Biol.* **58**, 509–522.

Hunter, J. R. and Zweifel, J. R. (1971). Swimming speed, tail beat frequency, tail beat amplitude and size in jack mackerel, *Trachurus symmetricus* and other fishes. *Fish. Bull.* **69**, 253–266.

Jayne, B. C. and Lauder, G. V. (1993). Red and white muscle activity and kinematics of the escape response of bluegill sunfish during swimming. *J. Comp. Physiol. A* **173**, 495–508.

Jayne, B. C. and Lauder, G. V. (1995). Are muscle fibers within fish myotomes activated synchronously? Patterns of recruitment within deep myomeric musculature during swimming in largemouth bass. *J. Exp. Biol.* **198**, 805–815.

Johnston, I. A., Franklin, C. E. and Johnson, T. P. (1993). Recruitment patterns and contractile properties of fast muscle fibres isolated from rostral and caudal myotomes of the short-horned sculpin. *J. Exp. Biol.* **185**, 251–265.

Josephson, R. K. (1985). Mechanical power output from striated muscle during cyclical contraction. *J. Exp. Biol.* **114**, 493–512.

Katz, S. L., Shadwick, R. E. and Rapoport, H. S. (1999). Muscle strain histories in swimming milkfish in steady and sprinting gaits. *J. Exp. Biol.* **202**, 529–541.

Moi, C. R. and Breddels, P. A. (1982). Ultrasound velocity in muscle. *J. Acoust. Soc. Am.* **71**, 455–461.

Rayner, M. D. and Keenan, M. J. (1967). Role of red and white muscles in the swimming of the skipjack tuna. *Nature* **214**, 392–393.

Rome, L. C., Choi, I. H., Lutz, G. and Sosnicki, A. (1992). The influence of muscle temperature on the fast swimming scup. I. Shortening velocity and muscle recruitment during swimming. *J. Exp. Biol.* **163**, 259–279.

Rome, L. C., Funke, R. P. and Alexander, R. McN. (1990). The influence of temperature on muscle velocity and sutained performance in swimming carp. *J. Exp. Biol.* **154**, 163–178.

Rome, L. C., Loughna, P. T. and Goldspink, G. (1984). Muscle fibre activity in carp as a function of swimming speed and muscle temperature. *Am. J. Physiol.* **247**, R272–R279.

van Leeuwen, J. L., Lankheet, M. J. M., Akster, H. A. and Osse, J. W. M. (1990). Function of red axial muscles in carp (*Cyprinus carpio* L.): recruitment and normalized power ouput during swimming in different modes. *J. Zool., Lond.* **220**, 123–145.

Videler, J. J. and Hess, F. (1984). Fast continuous swimming of two pelagic predators, saithe (*Pollachius virens*) and mackerel (*Scomber scombrus*): a kinematic analysis. *J. Exp. Biol.* **109**, 209–228.

Wakeling, J. M. and Johnston, I. A. (1998). Muscle power output limits fast-start performance in fish. *J. Exp. Biol.* **201**, 1505–1526.

Wakeling, J. M. and Johnston, I. A. (1999). White muscle strain in the common carp and red to white muscle gearing ratios in fish. *J. Exp. Biol.* **202**, 521–528.

Wardle, C. S. and Videler, J. J. (1993). The timing of the electromyogram in the lateral myotomes of mackerel and saithe at different swimming speeds. *J. Fish Biol.* **42**, 347–359.

Wardle, C. S., Videler, J. J., Arimoto, T., Franco, J. M. and He, P. (1989). The muscle twitch and the maximum swimming speed of giant bluefin tuna, *Thunnus thynnus* L. *J. Fish Biol.* **35**, 129–137.

Webb, P. W. (1975). Hydrodynamics and energetics of fish propulsion. *Bull. Fish. Res. Bd Can.* **190**, 1–159.

Webb, P. W. (1978). Hydrodynamics: Nonscombroid fish. In *Fish Physiology*, vol. VII (ed. W. S. Hoar and D. J. Randall), pp. 190–239. New York, London: Academic Press.

Webb, P. W., Kostecki, P. T. and Stevens, E. D. (1984). The effects of size and swimming speed on locomotion kinematics of rainbow trout. *J. Exp. Biol.* **109**, 77–95.

Westerfield, M., McMurray, J. V. and Eisen, J. S. (1986). Identified motorneurones and their innervation of axial muscles in the zebrafish. *J. Neurosci.* **6**, 2267–2277.